08

Theoretical study of the decoration of the fullerene C_{60} with iron oxides

© A.R. El Zanin, S.V. Boroznin, I.V. Zaporotskova, N.P. Boroznina

Volgograd State University,
400062 Volgograd, Russia
e-mail: aelzanin@volsu.ru

Received December 9, 2025
Revised December 9, 2025
Accepted December 9, 2025

Composite materials based on the fullerenes and metal oxides have a great potential for applications in different fields of science and technique, in particular, for the formation of the selective and sensitive gas sensors, additives for a transformer oil, systems for the address drug delivery and diagnosis of diseases. Such a circumstance requires clarification of the mechanisms of formation of such composite materials. In the present work the processes of the decoration of the fullerene C_{60} with iron oxide molecules of various valences: FeO, Fe_2O_3, Fe_3O_4 were studied. Quantum chemical modeling was carried out using the methods of density functional theory at the level of theory B3LYP/6-31G. The adsorption parameters for each of the considered adsorption positions were determined and the most energetically preferred ones were identified. Additional geometry optimization was performed for configurations corresponding to the condition of minimum potential energy. The effect of the modification procedure under consideration on the band gap and charge distribution was studied. It is found that the band gap decreases for all the cases under consideration, and the electron density shifts from the iron atoms of the oxides to the carbon atoms of the fullerene. Based on the approaches of band theory, possible mechanisms leading to a decrease in the band gap are discussed. The results presented in this paper open up a new perspective on the formation of composite materials based on fullerenes and metal oxides.

Keywords: fullerenes, iron oxides, density functional theory, charge distribution, band gap.

DOI: 10.61011/TP.2026.05.63523.309-25

Introduction

Composite materials fabricated from carbon nanomaterials and metal oxides are currently in the focus of attention of researchers globally due to their unique physico-chemical properties, making them very promising for application in various fields of science and technology [1–3]. The emergence of new mechanical, adsorption, electrophysical, and optical properties in hybrid composite materials that are not found in the initial components is associated with the synergistic effects. The know-how aimed at creating flexible nanoelectronics and optoelectronics devices based on modified carbon nanomaterials look especially promising. It is the carbon platform that is rightly considered as one of the most promising one for creating new high-tech devices [4,5]. In such devices, the carbon base provides basic electronically conductive and mechanical (strength and flexibility) properties, while the metal oxide component raises the functionality for specific applications in one way or another, for example, it provides higher selectivity when detecting gaseous substances in gas sensors [6–10], increases specific power and capacitance of supercapacitors [11–13] or allows converting most of the solar spectrum into electricity in photovoltaic cells [14–16]. Developments for biomedical applications, namely targeted drug delivery systems, are also very promising: modification of carbon nanostructures with metal oxides allows releasing a drug when a magnetic field is applied [17,18], laser radiation is applied [19], which increases the effectiveness of therapy and minimizes the possible negative effects of drugs on healthy cells. Also, such systems can be used not only for treatment, but also in diagnostics, in particular, by means of MRT; such a combination of diagnostics and treatment in one approach, one technology, is called theranostics [20].

Fullerenes are a group of carbon nanomaterials in the form of convex polyhedra, the vertices of which contain carbon atoms in a state of sp^2-hybridization. The surface of fullerenes consists of pentagons and hexagons, and the most stable structures are those that obey the so-called isolated pentagon rule, i.e. structures where each pentagon is surrounded on all sides by hexagons and, accordingly, adjacent pentagons are absent [21]. Nonconventional fullerenes are distinguished separately, which, along with pentagonal and hexagonal fragments, can contain quadrilaterals, heptagons, etc. [22,23]; the stability of such structures is disputable, although theoretical analysis has shown that some small fullerenes can be stable in just such forms [24]. The introduction of impurities of various nature makes it possible to control the physico-chemical properties of fullerenes, which can be useful for various practical applications [25,26]. The first experimentally obtained fullerene was C_{60}; in 1985, it was synthesized by laser evaporation and identified by mass spectroscopy [27]. Kroto, Smalley, and Curl, who were part of the research team engaged in this project, were subsequently awarded the Nobel Prize in Chemistry. It should be noted that the possibility of the existence of such a structure was proved by theoretical methods much earlier: in 1970 a paper on this topic was published by

the Japanese researcher Osawa [28], and in 1973 — Soviet scientists Bochvar and Halpern [29]. C_{60} and C_{70} fullerenes are today fabricated in an industrial scale; it is these two fullerenes that are contained in the largest quantities in fullerene-containing carbon black formed during electric arc discharge; the volume of the global fullerene market in 2021 amounted to 522.6 million dollars [30]. Thus, C_{60} fullerene is a commercially demanded product today, and the search for new promising materials based on it is a very pressing issue.

Hybrid composite materials based on C_{60} fullerene and metal oxides are of great research interest; previously, the prospects of composites based on carbon nanomaterials and metal oxides in general were discussed, then we will consider developments based directly on C_{60} fullerene. In [31], a quantum chemical study of the adsorption activity of composites based on fullerene C_{60} and oxides of copper (I) Cu_2O, zinc ZnO and nickel NiO was carried out with respect to nitric oxide (IV) NO_2 and carbon monoxide CO. The analysis was performed within the density functional theory using B97D functional and basis set 6-311G(d,p). The charge distribution was analyzed within NBO scheme. The chemical properties of the formed bonds and their relative strength were evaluated using Bader theory methods. It was found that adsorption energy of gas molecules on the surface of modified C_{60} fullerene is significantly higher than on the surface of pure fullerene, which evidences the formation of a stronger chemical bond between the interacting objects. It is also expected that these complexes have sufficiently high optical and electrical sensitivity to gases, including NO_2 and CO. This allows us to conclude that the proposed materials are promising for creating gas sensors and adsorbents of harmful gases. The study [32] also outlines the option of creating CO sensor based on C_{60}/ZnO nanosystem. In this study, the analysis performed using density functional theory methods was aimed at establishing the stability and response of C_{60} fullerenes coated with ZnO using Raman spectroscopy. It was found that the zinc oxide coating on the fullerene surface is heterogeneous and consists of localized $(ZnO)_n$ clusters of different sizes. Different coating morphology options provide various mechanisms of electron density transfer both from the carbon component to the metal oxide component and in the opposite direction. It was found that there is a strong interaction between Zn atoms of the oxide coating and CO molecules. The presence of a metal oxide layer greatly enhances the system response when using Raman spectroscopy at frequencies corresponding to C_{60}. But more interesting from a practical standpoint is a higher intensity of peaks corresponding to CO molecules adsorbed on ZnO surface. The authors declare that this clearly allows to consider the examined carbon nanostructures as ultra-sensitive carbon monoxide detectors. To describe the phenomena observed in the model experiment, the term „fullerene-enhanced Raman scattering“ was first introduced in this paper. It was noted that CO detection based on Raman spectroscopy methods complements previous studies, which mainly analyzed changes in the electrical resistance of zinc oxide/nanocarbon samples during CO adsorption. The study [33] described the potential use of C_{60} fullerene and iron oxide nanoparticles as a transformer oil additive. The study by dielectric spectroscopy methods allowed to find out that the dielectric response of magnetic nanoparticles prevails in the dielectric spectrum of the resulting hybrid compositions of transformer oil. It is also assumed that the addition of fullerenes to transformer oils increases their stability and thus prolongs their service life. This is explained by binding of free radicals formed during operation by means of fullerenes. The study [34] discussed the use of C_{60}/MnO_x heterostructure as the basis for some spintronics components. The physical features inherent in this system make it possible to capture spin-polarized charge carriers when an external electric voltage is applied or when it is exposed to laser radiation, whereas exposure to an external magnetic field allows to control the storage time of the spin-polarized charge carriers. This opens up new possibilities for designing memory elements based on the principles of spintronics. In the works [35,36], the effectiveness of using a targeted drug delivery system based on C_{60} fullerene, decorated with iron oxide nanoparticles and coated with polyethylene glycol, for the purposes of oncology theranostics was investigated. Hematoporphyrin and methanol-based ester and folic acid were considered as therapeutic drugs. The presented technological platform also provides diagnostics using MRT methods.

Thus, practical applicability of composites based on C_{60} fullerene and metal oxides, in particular, iron oxides, leaves no doubts. However, the impact of iron oxide specific type on the structure and properties of the formed composite has not been studied in the literature so far. The iron atoms in oxides are known to have valences II and III, and, thus, three oxides are distinguished: FeO (II), Fe_2O_3 (III) and Fe_3O_4 (II, III). Based on the differences in their physico-chemical properties, it may be suggested that they interact with carbon nanostructures in different ways. This study was aimed at investigating the processes of surface modification of C_{60} fullerene by introducing iron oxides FeO, Fe_2O_3, Fe_3O_4, and assessing the impact of this procedure on physical and chemical properties of the examined nanosystem.

1. Materials and methods

Quantum chemical modeling was carried out in Orca [37] software package using density functional theory methods with hybrid B3LYP functional and 6-31G basic set [38,39]. Calculations performed at the proposed level of theory made it possible to obtain results comparable in accuracy with the experiment as was proved based on the analysis of a fairly large sample of physical quantities measured in model and real experiments [39,40]. Density functional theory, thus, can be considered as a fairly reliable approach, while at the same time being optimal

in terms of the required computation capacity [41–43]. It is based on the well-known Kohn-Sham equation. Let's define the type of functional for the average energy as follows:

$$E[n] = \left\langle \Psi[n] | (\hat{T} + \hat{U} + \hat{V}_{ext}) | \Psi[n] \right\rangle$$

$$= T + U + V_{ext} = T_S + V_H + V_{ext} + (T - T_S + U - V_H).$$

The last term in this expression stands for the contribution of the exchange-correlation energy:

$$V_{XC} = (T - T_S + U - V_H).$$

The pairwise difference included in this expression in total gives the specified energy value. The first difference is between the kinetic energies of interacting and free particles, and the second difference is between the energies of the Coulomb interaction and Hartree.

For better certainty, it is possible to rewrite the Kohn-Sham functional with an indication of the functional dependence of the terms before proceeding to specific calculations:

$$E_{KX}[n] = T_S[n] + V_H[n] + V_{ext}[n] + V_{XC}[n].$$

We will set the appropriate ratios to perform variation:

$$\frac{\delta E_{KS}}{\delta \Psi_{i\sigma}(r)} = \frac{\delta T_S}{\delta \Psi_{i\sigma}(r)}$$

$$+ \left[\frac{\delta V_H}{\delta n(r)} + \frac{\delta V_{est}}{\delta n(r)} + \frac{\delta V_{XC}}{\delta n(r)} \right] \frac{\delta n(r)}{\delta \Psi_{i\sigma}(r)} = 0,$$

$$\frac{\delta T_S}{\delta \Psi_{i\sigma}(r)} = -\frac{1}{2} \nabla^2 \Psi_{i\sigma}(r).$$

The introduction of the Lagrange multiplier (denoted below $\varepsilon_{i\sigma}$) sets the normalization condition. Given all the above transformations, the Kohn-Sham equation may be written as follows:

$$-\frac{1}{2} \nabla^2 \Psi_{i\sigma}(r) + v_{KS}(r) \Psi_{i\sigma}(r) = \varepsilon_{i\sigma} \Psi_{i\sigma}(r).$$

This equation coincides in appearance with the single-particle Schrodinger equation, which describes the behavior of a particle in a self-consistent potential, given by the expression

$$v_{KS}(r) = v_{ext}(r) + v_H(r) + v_{XC}(r),$$

$$v_{ext}(r) = \int dr' \frac{n(r')}{|r - r'|},$$

$$v_{XC}(r) = \frac{\delta V_{XC}}{\delta n(r)},$$

$$n(r) = \sum_{i\sigma} |\Psi_{i\sigma}(r)|^2.$$

Previously, improved geometries of the considered iron oxides were obtained, which assumed the selection of such geometric parameters (bond lengths, valence and torsion angles) at which the total energy of the system would be minimal (Fig. 1). All considered systems were featuring a „singlet“ multiplexity. The step-by-step approximation of iron oxides was performed along a perpendicular to the fullerene surface in five positions (Fig. 2): 1) above the carbon atom, 2) above the center of the single bond, 3) above the center of the double bond, 4) above the center of the pentagon, 5) above the center of the hexagon. In case of FeO and Fe_2O_3 oxides the approximation was accomplished using both, iron atom and oxygen atom. In case of Fe_3O_4 iron atoms of different valences were used in the approximation. At each step of the approximation, the distance between the carbon atom (or fictitious pseudo-atom) and the oxide atom that was being approximated in a particular case and the total energy of the system were recorded. The obtained data allowed to plot the profiles of the potential energy surface (PPES), on the basis of which the analysis of the energy preference of a particular adsorption position and the option of approaching the oxide by a particular atom was carried out. After determining the most energetically advantageous adsorp-

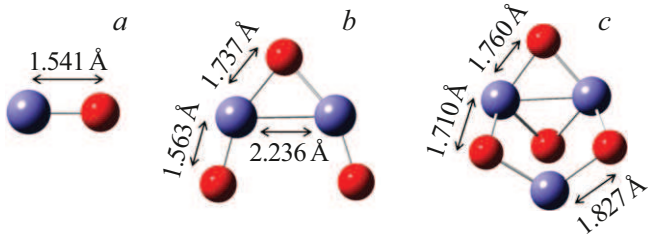

Figure 1. Optimized geometries of iron oxides FeO (*a*), Fe_2O_3 (*b*), Fe_3O_4 (*c*) with annotated bond lengths.

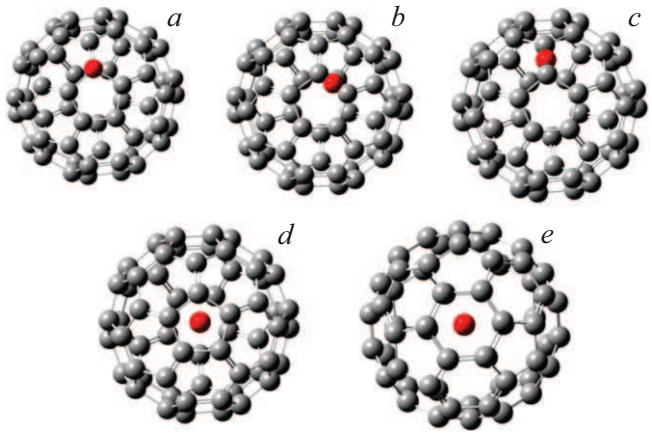

Figure 2. The considered positions of the iron oxides adsorption on the surface of C_{60} fullerene, indicated by a red fictitious pseudoatom: above the carbon atom (*a*), above the center of the single bond (*b*), above the center of the double bond (*c*), above the center of the pentagon (*d*), above the center of the hexagon (*e*).

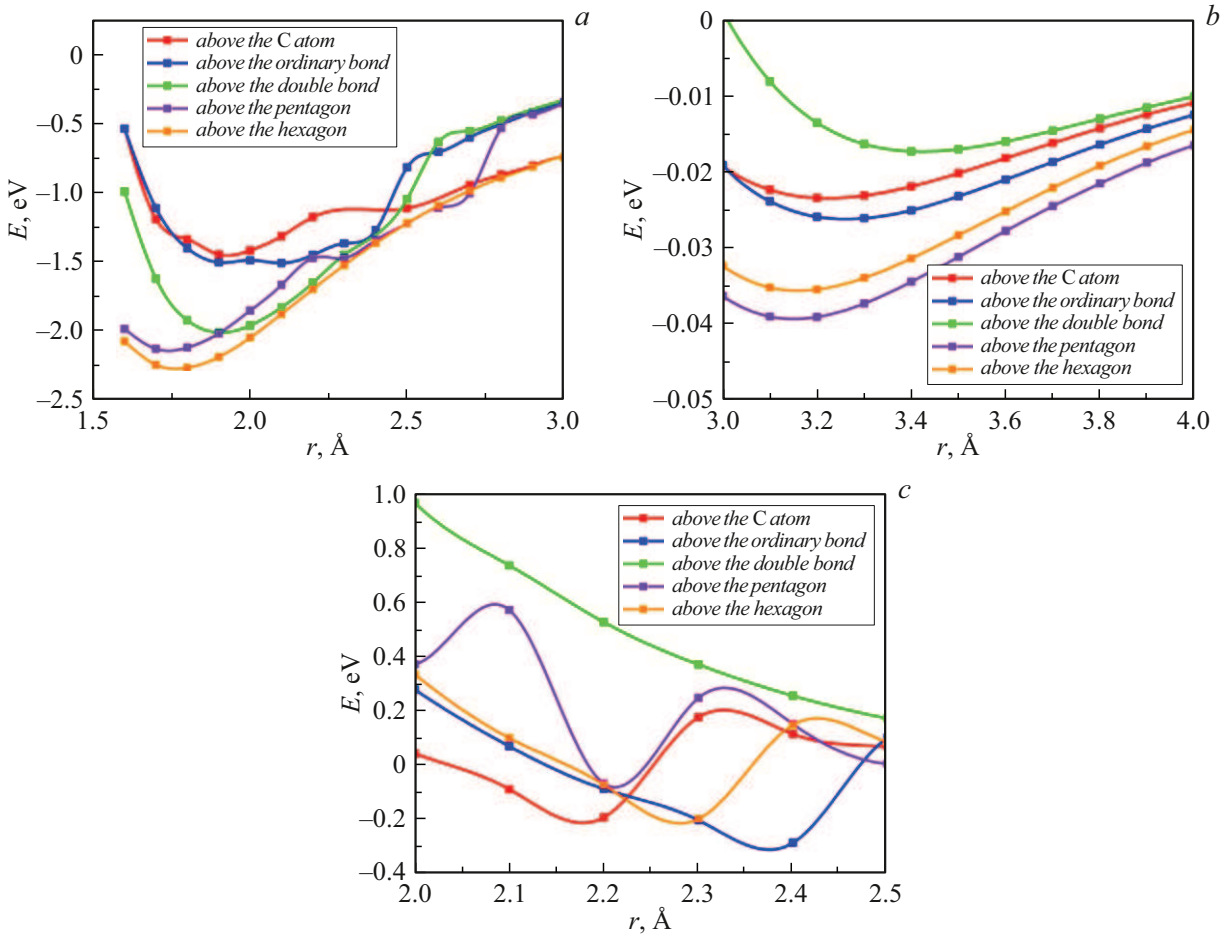

Figure 3. PPES of interaction between C_{60} fullerene and iron oxide FeO in the oxide approximation by the iron atom (*a*) and oxygen atom for the distances from 3.0 to 4.0 Å (*b*) and from 2.0 to 2.5 Å (*c*).

tion positions, the geometries of the systems were re-optimized.

Partial atomic charges were calculated based on the Mulliken scheme [44,45]. It represents the charge on an atom as the difference between its atomic number and the sum of the populations of the basic functions centered on this atom and the populations of overlap with the basic functions centered on other atoms. The band gap ΔE_g was determined as the difference between the energy of the lowest unoccupied molecular orbital E_{LUMO} and the energy of the the highest occupied molecular orbital E_{HOMO}. Full (DOS) and partial (PDOS) densities of states were plotted using GaussSum software [46].

2. Results and discussion

Let's consider separately the options for decorating fullerene with each type of iron oxide. The obtained PPES for the case of interaction of C_{60} and FeO (Fig. 3) allowed us to establish that the most energetically advantageous process is the adsorption of iron oxide FeO in its surface approximation by an iron atom (Fig. 3, *a*). The most probable position of adsorption here is the position above the center of the hexagon: in this case, the adsorption energy is 2.263 eV, and the adsorption distance is 1.8 Å. For the rest of positions, the adsorption energy ranges from 1.446 to 2.127 eV, and the adsorption distance is — in the range from 1.7 to 2.1 Å. Here, in case of FeO approximation by oxygen atom, physical adsorption is first observed (Fig. 3, *b*), at which the adsorption distance ranges from 3.2 to 3.4 Å, and the adsorption energy — from 0.017 to 0.039 eV depending on the adsorption position, and upon further approach, after overcoming potential barriers with heights from 0.125 to 0.286 eV, a stronger interaction is observed (Fig. 3, *c*), with the adsorption distance ranging from 2.2 to 2.4 Å, and the adsorption energy being from 0.070 to 0.298 eV. An exception in this context is the position of adsorption above the center of the double bond, where no additional minima are observed at distances less than the physical adsorption distance of 3.4 Å.

In case of surface modification of C_{60} with iron oxide Fe_2O_3, when it is approximated by an iron atom (Fig. 4, *a*), a strong chemical bond is formed, and the most energetically advantageous position of adsorption is the position

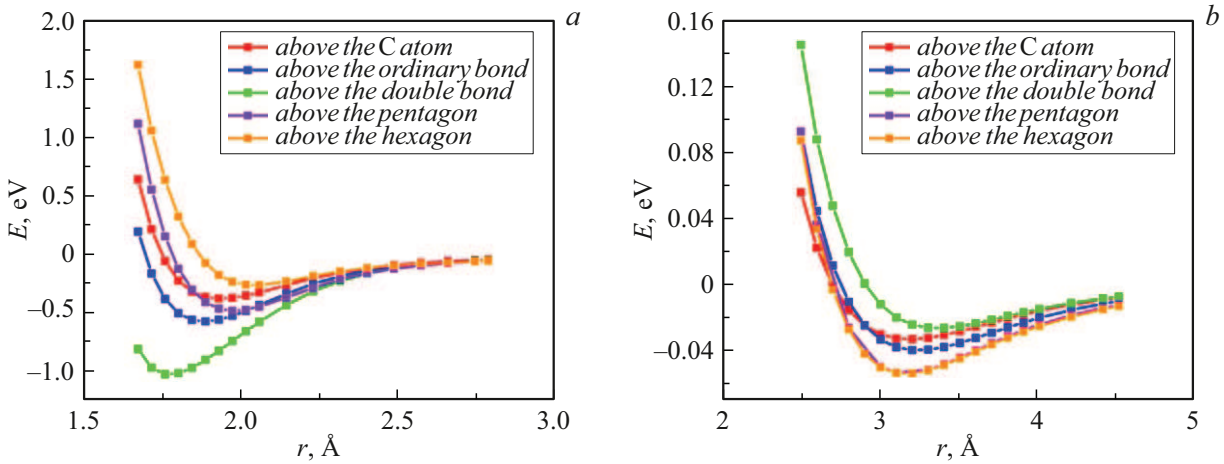

Figure 4. PPES of interaction of C_{60} fullerene and Fe_2O_3 iron oxide in approximation of the oxide with iron atom (*a*) and oxygen atom (*b*).

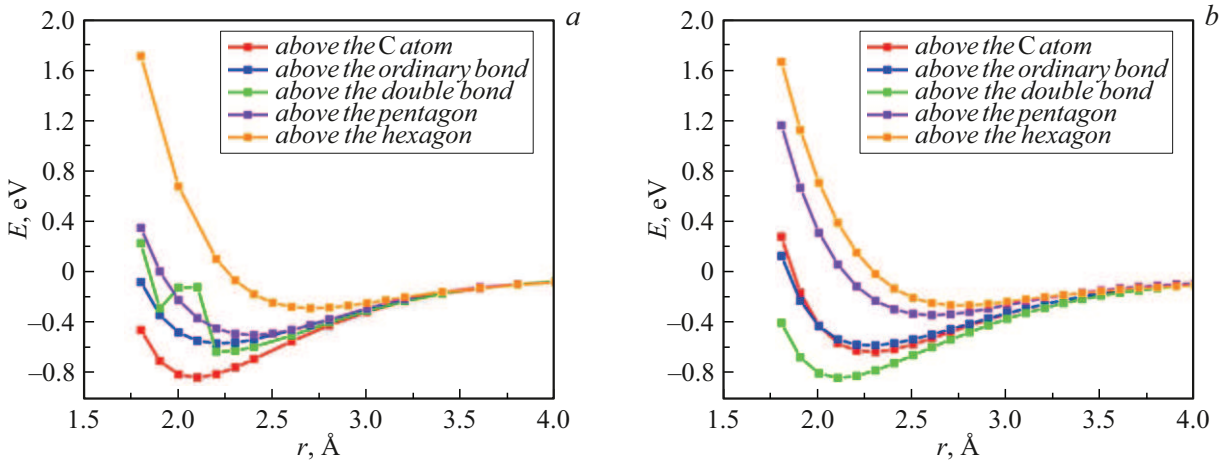

Figure 5. PPES of interaction of C_{60} fullerene and Fe_3O_4 oxide in approximation by a 2-valence (*a*) and 3-valence (*b*) iron atoms.

above the center of the double bond: the adsorption energy in this modification variant is 1.025 eV, and the adsorption distance is — 2.1 Å. In other positions the adsorption energy has values from 0.265 to 0.575 eV, and adsorption distances — from 2.4 to 2.8 Å. When iron oxide Fe_2O_3 is approximated by an oxygen atom (Fig. 4, *b*), the only possible process is physical adsorption, observed in all the considered adsorption positions. At that, the adsorption distance makes from 3.1 to 3.4 Å, and adsorption energy — from 0.026 to 0.053 eV.

The adsorption of iron oxide Fe_3O_4 on the surface of fullerene C_{60} can be carried out at any of the considered adsorption positions both in the case of oxide approximation by a divalent iron atom (Fig. 5, *a*) and by a trivalent iron atom (Fig. 5, *b*). In both cases the adsorption has a nature of chemical sorption. The energetically most advantageous position of adsorption when the oxide is approximated by a divalent iron atom is the position above the carbon atom: the adsorption energy in this case is 0.840 eV, and the adsorption distance is — 2.1 Å. For the rest adsorption positions given this version of the oxide approximation, the adsorption energy ranges from 0.292 to 0.636 eV, and the adsorption distance — from 2.2 to 2.7 Å. In case of approximation of the oxide by a trivalent iron atom, the energetically most advantageous position of adsorption is the position above the center of the double bond: the adsorption energy in this case is 0.838 eV, the adsorption distance — 2.1 Å. For the rest of positions, the adsorption energy is from 0.263 to 0.632 eV, and the adsorption distance — from 2.3 to 2.8 Å.

After determining the most energetically beneficial adsorption positions for the corresponding configurations, the geometry was re-optimized (Fig. 6).

Let's consider how the electron-energy properties of decorated nanosystems have changed compared to the original C_{60} fullerene. The band gap of the initial pure fullerene is equal 2.996 eV, and the energies E_{LUMO} and E_{HOMO} make -3.286 eV and -6.282 eV respectively. In DOS graph (Fig. 7, *a*) for the pure fullerene C_{60} in the range of energies from -8 to -2 eV four symmetric peaks are

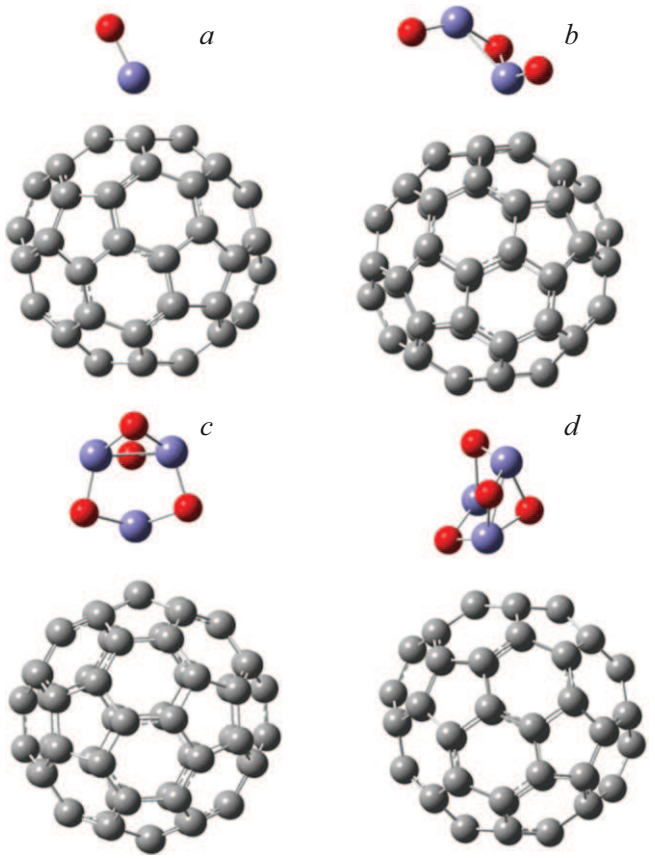

Figure 6. re-optimized geometries of nanostructures C_{60}/FeO (*a*), C_{60}/Fe_2O_3 (*b*), C_{60}/Fe_3O_4 when a 2-valence (*c*) and 3-valence (*d*) iron atoms are located near the fullerene surface, where the adsorption positions comply with the potential energy minimum.

observed, two of which belong to the valence band, another two peaks belong to the conduction band. As a result of adsorption of FeO the band gap decreases by 41.7 % and becomes equal 1.747 eV. This is caused by the two observed processes: decrease of the bottom of the conduction band and raise of the top of the valence band. Since the value of E_{LUMO} for the considered system is equal -3.703 eV, which indicates a decrease in the conduction band bottom; the value E_{HOMO} makes -5.450 eV, which indicates, in turn, a raise in the valence band top. By analysing PDOS graph (Fig. 7, *b*) we may conclude that the energy levels forming the top of the valence band are mainly of an impurity kind, while the levels of the conduction band bottom are predominantly intrinsic. The change in the band gap when modifying fullerene C_{60} with Fe_2O_3 iron oxide is weakest compared to other reviewed cases: the decrease in the band gap with this modification option is 17.6 %. The absolute value of the band gap of C_{60}/Fe_2O_3 is 2.468 eV. Here, in contrast to the previous case, two processes are observed having opposite effect on the band gap: lowering the top of the valence band, leading to an increase in the band gap, and at the same time lowering the bottom of the conduction band, which helps to reduce the band gap. Yet, the first process is less pronounced than the second, so, eventually, the band gap decreases. E_{LUMO} is equal -3.868 eV, E_{HOMO} is equal -6.336 eV. The data analyzed in PDOS graph (Fig. 7, *c*) show that both the bottom of the conduction band and the top of the valence band are formed by both impurity and intrinsic energy levels, and the contribution of impurity levels is less significant compared to intrinsic levels. The adsorption of Fe_3O_4 with its approximation by a divalent iron atom leads to a decrease in the band gap by 30.4 %, to 2.085 eV. Moreover, here, as in case of FeO adsorption, a decrease in the band gap is facilitated by both a decrease in the bottom of the conduction band and a raise in the top of the valence band: the value E_{LUMO} is -3.917 eV, E_{HOMO} value is -6.002 eV. The levels of the bottom of the conduction band are predominantly impurity, while the levels of the valence band top are — intrinsic, which follows from the analysis of PDOS graph for the considered system (Fig. 7, *d*). Another case of Fe_3O_4 adsorption on the surface of C_{60} fullerene in which the oxide was approximated by a trivalent iron atom, is notable for the fact that the decrease in the band gap is expressed to the greatest extent and amounts to 45.4 %, the absolute value of this indicator is 1.637 eV. As in previously considered case of adsorption of the same oxide, but when approximated by a divalent iron atom, or modification of a fullerene with FeO oxide, a decrease in the band gap is associated with two processes, namely, a decrease in the bottom of the conduction band and an increase in the top of the valence band. Here, the value E_{LUMO} is equal -3.706 eV, and the value of E_{HOMO} is equal -5.343 eV. Based on the analysis of PDOS graph (Fig. 7, *e*), it was found that with a similar modification variant, a situation is observed opposite to the previously considered case for the same iron oxide

Fe_3O_4, but close to the surface with a divalent iron atom, in the sense that the top levels of the valence band they are mainly of an impurity type, and the bottom levels of the conduction band, on the contrary, are predominantly intrinsic. In all considered cases of modification of C_{60} by various iron oxides, a violation of the symmetry of peaks on DOS graph characteristic of pure C_{60} fullerene was observed.

Let us now study the charge distribution in composites based on fullerene C_{60} and various types of iron oxides. First, it should be noted that in the isolated state in iron oxide FeO the charge on the iron atom is 0.392, in Fe_2O_3 the charge on the iron atom that was approximated is 0.712, in Fe_3O_4, the charge on the divalent iron atom is 0.874, on the trivalent, respectively, 0.893. In all the modified nanosystems considered, a shift in electron density from iron atoms to carbon atoms is observed. For C_{60}/FeO composite the charge on the iron atom is 0.733; the charge on the carbon atoms forming the hexagon vary from -0.089 to -0.053. For C_{60}/Fe_2O_3 composite the charge on the iron atom is 0.746, while on the carbon atoms forming the double bond, the charge is equal -0.238 and -0.186. For C_{60}/Fe_3O_4 composites, the charge value on the iron atom is 1.045 when approximated by a divalent iron atom,

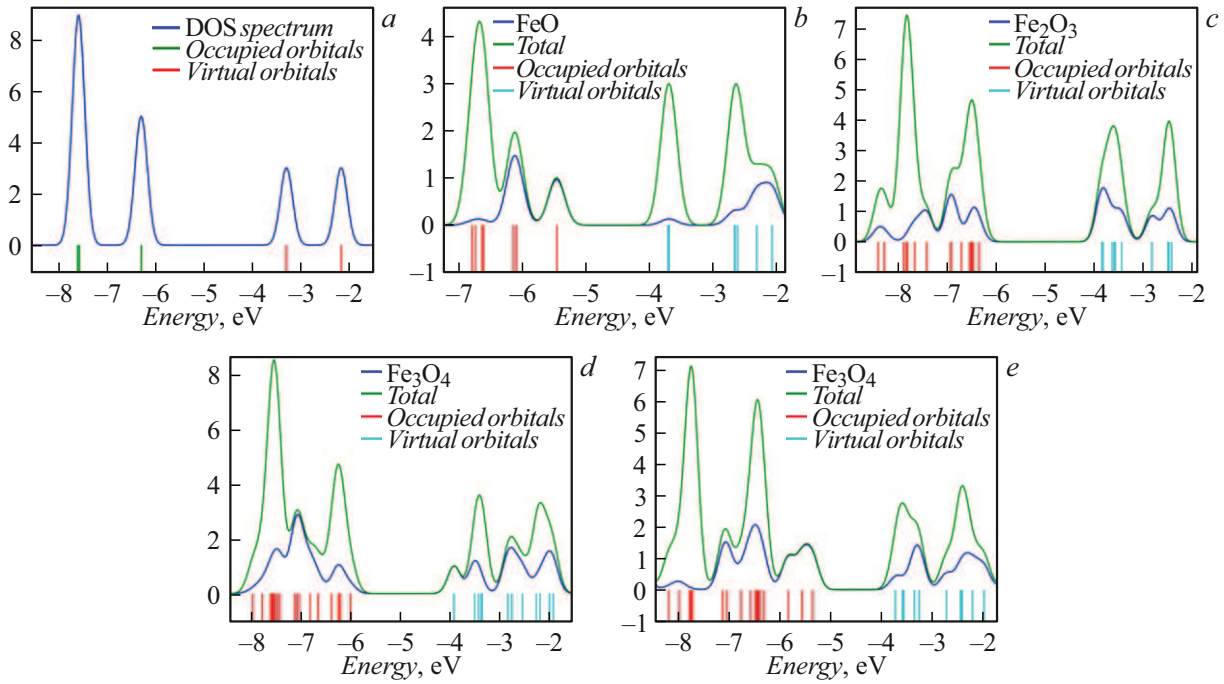

Figure 7. DOS for pure fullerene C_{60} (*a*), DOS and PDOS for the composites C_{60}/FeO (*b*), C_{60}/Fe_2O_3 (*c*), C_{60}/Fe_3O_4, obtained from approximation of the oxide by divalent (*d*) and trivalent (*e*) atoms of iron.

and 1.021 — when approximated by a trivalent iron atom. Moreover, for a system formed during the approximation of an oxide by a divalent iron atom, the charge on the carbon atom closest to the iron oxide atom is −0.301; it is also interesting to note that an additional shift in electron density is observed to the neighboring carbon atom, which gets a charge of −0.150. For the system obtained by approximating the oxide with a trivalent iron atom, the charges on the carbon atoms forming the double bond are −0.226 and −0.217.

Conclusion

Thus, as part of the study, quantum chemical modeling of the decoration of C_{60} fullerene with iron oxides FeO, Fe_2O_3, Fe_3O_4 was carried out, the energetically most advantageous adsorption positions for optimized geometries of composite nanosystems were determined, where the adsorption positions corresponded to the condition of minimum potential energy, parameters characterizing electron-energy properties and charge distribution were studied.

Due to the analyzed data we could find out that the adsorption of all iron oxides considered on the surface of C_{60} fullerene is energetically most beneficial when the oxides were approximated by iron atoms, in this case, the formation of strong chemical bonds was observed, while when the oxides were approximated by oxygen atoms, physical sorption was a predominant mechanism. Nevertheless, in case of FeO oxide, the formation of a chemical bond is possible, but such a bond is still characterized by an energy an order of magnitude lower than for variants corresponding to the approximation of this oxide by the iron atom. The highest adsorption energy is observed for C_{60}/FeO system at the adsorption position above the center of the hexagon, respectively, the bond between the carbon and metal oxide components in such a composite is the strongest compared to other systems considered. The highest value of the adsorption energy in C_{60}/Fe_3O_4 systems practically coincides with both the divalent iron atom (0.840 eV) and the trivalent iron atom (0.838 eV), although the position of adsorption in these two cases will be different.

The decoration of C_{60} fullerene with iron oxides leads to a decrease in the band gap by an amount from 17.6 % to 45.4 %, depending on the type of oxide. This pattern is caused by both a decrease in the bottom of the conduction band and an increase in the top of the valence band. The exception is C_{60}/Fe_2O_3 composite where there is a decrease in the top of the valence band — a process that has the opposite effect and, in general case, leads to an increase in the band gap; however, in this system, the process of lowering the bottom of the conduction band is more pronounced, and, ultimately, the band gap also declines.

The electron density in all the considered composites is shifted from iron atoms to carbon atoms, while the highest absolute charge on an iron atom was observed in C_{60}/Fe_3O_4, obtained during the approximation of oxide by a divalent iron atom, and was 1.045. However, if we consider the relative change in the charge value compared to the isolated state of the oxide, then the greatest change is observed in

the system C_{60}/FeO, where the charge on the iron atom increases by 87.0%.

The results obtained demonstrate aspects of the formation of nanostructures based on C_{60} fullerene and iron oxides that had not been previously outlined in the literature. Knowing the processes accompanying the fabrication of such composites can be extremely useful for creating new materials for optoelectronics, gas sensors, and biomedical systems for a targeted drug delivery.

Funding

This study was carried out under state assignment of the Ministry of Science and Higher Education of the Russian Federation (project „FZUU-2023-0001“).

Conflict of interest

The authors declare that they have no conflict of interest.

References

[1] P. Bijesh, V. Selvaraj, V. Andal. Mater. Today: Proc., **55**, 212 (2022). DOI: 10.1016/j.matpr.2021.06.163
[2] N. Devi, S. Sahoo, R. Kumar, R.K. Singh. Nanoscale, **13** (27), 11679 (2021). DOI: 10.1039/D1NR01134K
[3] H.A.A. Jamjoum, K. Umar, R. Adnan, M.R. Razali, M.N. Mohamad Ibrahim. Front. Chem., **9**, 752276 (2021). DOI: 10.3389/fchem.2021.752276
[4] J. Wu, H. Lin, D.J. Moss, K.P. Loh, B. Jia. Nat. Rev. Chem., **7** (3), 162 (2023). DOI: 10.1038/s41570-022-00458-7
[5] A. Tundwal, H. Kumar, B.J. Binoj, R. Sharma, G. Kumar, R. Kumari, A. Dhayal, A. Yadav, D. Singh, P. Kumar. RSC Adv., **14** (14), 9406 (2024). DOI: 10.1039/D3RA08312H
[6] M. Sinha, S. Neogi, R. Mahapatra, S. Krishnamurthy, R. Ghosh. Sens. Act. B: Chem., **336**, 129729 (2021). DOI: 10.1016/j.snb.2021.129729
[7] S. Chang, M. Yang, R. Pang, L. Ye, X. Wang, A. Cao, Y. Shang. Appl. Surf. Sci., **579**, 152172 (2022). DOI: 10.1016/j.apsusc.2021.152172
[8] M. Davydova, P. Ashcheulov, A.P. Papavlu, A. Laposa, A. Taylor, J. Kroutil, T. Lippert. Sens. Act. A: Phys., **389**, 116525 (2025). DOI: 10.1016/j.sna.2025.116525
[9] W. Photaram, M. Liangruksa, M. Aiempanakit, C. Suwanchawalit, A. Wisitsoraat, J. Sukunta, S. Laksee, C. Siriwong. Appl. Surf. Sci., **595**, 153510 (2022). DOI: 10.1016/j.apsusc.2022.153510
[10] A.R. El Zanin, S.V. Boroznin, I.V. Zaporotskova, N.P. Boroznina, N. Venkatesh, G. Murugadoss. Sens. Act. A: Phys., **389**, 116565 (2025). DOI: 10.1016/j.sna.2025.116565
[11] B. Tale, K.R. Nemade, P.V. Tekade. Polym.-Plast. Technol. Mater., **60** (7), 784 (2021). DOI: 10.1080/25740881.2020.1851378
[12] S. Ramesh, S. Khandelwal, K.Y. Rhee, D. Hui. Compos. Part B: Eng., **138**, 45 (2018). DOI: 10.1016/j.compositesb.2017.11.024
[13] P. Lin, Q. She, B. Hong, X. Liu, Y. Shi, Z. Shi, M. Zheng, Q. Dong. J. Electrochem. Soc., **157** (7), A818 (2010). DOI: 10.1149/1.3425624
[14] V.A. Milichko, A.S. Shalin, A.E. Kovrov, A.A. Krasilin, A.V. Vinogradov, P.A. Belov, I.S. Mukhin, C.R. Simovski. Phys.-Usp., **59** (8), 727 (2016). DOI: 10.3367/UFNe.2016.02.037703
[15] P. Jain, R.S. Rajput, S. Kumar, A. Sharma, A. Jain, B.J. Bora, P. Sharma, R. Kumar, M. Shahid, A.A. Rajhi, M. Alsubih, M.A. Shah, A. Bhowmik. ACS Omega, **9** (11), 12403 (2024). DOI: 10.1021/acsomega.3c07994
[16] K. Fatima, A.H. Pandith, T. Manzoor, A. Qureashi. ACS Omega, **8** (9), 8865 (2023). DOI: 10.1021/acsomega.3c00333
[17] C. Wu, K.L. Shi, Y. Zhang, W. Jiang. J. Magn. Magn. Mater., **465**, 114 (2018). DOI: 10.1016/j.jmmm.2018.05.066
[18] J.H. Choi, F.T. Nguyen, P.W. Barone, D.A. Heller, A.E. Moll, D. Patel, S.A. Boppart, M.S. Strano. Nano Lett., **7** (4), 861 (2007). DOI: 10.1021/nl062306v
[19] M. Zhang, W. Wang, Y. Cui, X. Chu, B. Sun, N. Zhou, J. Shen. Chem. Eng. J., **338**, 526 (2018). DOI: 10.1016/j.cej.2018.01.081
[20] S.M. Hosseini, J. Mohammadnejad, R. Najafi-Taher, Z.B. Zadeh, M. Tanhaei, S. Ramakrishna. ACS Appl. Bio Mater., **6** (4), 1323 (2023). DOI: 10.1021/acsabm.2c01000
[21] A.R. Khamatgalimov, V.I. Kovalenko. Russian Chemical Journal, **48** (5), 28 (2004) (in Russian).
[22] V.A. Brotsman, S.I. Troyanov. Chem. Commun., **60** (7), 893 (2024). DOI: 10.1039/D3CC05336A
[23] A. Muñoz-Castro. Chem. Phys. Lett., **857**, 141693 (2024). DOI: 10.1016/j.cplett.2024.141693
[24] L.A. Openov, A.I. Podlivaev, M.M. Maslov. Phys. Lett. A, **376** (45), 3146 (2012). DOI: 10.1016/j.physleta.2012.09.017
[25] A.R. El Zanin, S.V. Boroznin, I.V. Zporotskova, N.P. Boroznina. ZhTF, **94** (3), 410 (2024) (in Russian). DOI: 10.61011/JTF.2024.03.57379.299-23
[26] A.R. El Zanin, S.V. Boroznin, I.V. Zaporotskova. Nanosyst.: Phys. Chem. Math., **16** (3), 374 (2025). DOI: 10.17586/2220-8054-2025-16-3-374-385
[27] H.W. Kroto, J.R. Heath, S.C. O'Brien, R.F. Curl, R.E. Smalley. Nat., **318** (6042), 162 (1985). DOI: 10.1038/318162a0
[28] E. Osawa. Kagaku, **25**, 854 (1970).
[29] D.A. Bovchar, E.G. Galpern. DAN USSR, **209** (3), 610 (1973). (in Russian).
[30] M. Punetha, J. Bhagat, R. Pathak, S. Bhatt, P. Sanghani, V.D. Punetha. *Industrial Scale Production, Commercialization, and Global Market of Functionalized Carbon Nanostructures*. In: A. Barhoum, K. Deshmukh (eds). *Handbook of Functionalized Carbon Nanostructures* (Springer, Cham., 2024). DOI: 10.1007/978-3-031-32150-4_75
[31] S. Haghgoo, A.R. Nekoei. RSC Adv., **11** (28), 17377 (2021). DOI: 10.1039/D1RA02251B
[32] A. Zamudio-Ojeda, S.J. Guevara-Martínez, J.G. Rodríguez-Zavala, R.A. Guirado-López. Phys. Chem. Chem. Phys., **27** (26), 14113 (2025). DOI: 10.1039/D4CP04884A
[33] R. Cimbala, P. Havran, J. Király, M. Rajňák, J. Kurimský, M. Šárpataky, B. Dolník, K. Paulovičová. J. Mol. Liq., **359**, 119338 (2022). DOI: 10.1016/j.molliq.2022.119338
[34] T. Moorsom, M. Rogers, I. Scivetti, S. Bandaru, G. Teobaldi, M. Valvidares, M. Flokstra, S. Lee, R. Stewart, T. Prokscha, P. Gargiani, N. Alosaimi, G. Stefanou, M. Ali, F. Al Ma'Mari, G. Burnell, B.J. Hickey, O. Cespedes. Sci. Adv., **6** (12), eaax1085 (2020). DOI: 10.1126/sciadv.aax1085
[35] J. Shi, X. Yu, L. Wang, Y. Liu, J. Gao, J. Zhang, R. Ma, R. Liu, Z. Zhang. Biomaterials, **34** (37), 9666 (2013). DOI: 10.1016/j.biomaterials.2013.08.049

[36] J. Shi, L. Wang, J. Gao, Y. Liu, J. Zhang, R. Ma, R. Liu, Z. Zhang. Biomaterials, **35** (22), 5771 (2014). DOI: 10.1016/j.biomaterials.2014.03.071
[37] F. Neese. Faraday Discussions, **254**, 295 (2024). DOI: 10.1039/D4FD00056K
[38] L.V. Kozhitov, I.V.Zaporotskova, D.G. Muratov, N.P. Boroznina, A.V. Popkova, S.V. Borosin, E.V. Yakushko. *Sintez, svoistva i modelirovaniye metallouglerodnykh nanokompositov* (Volgogradsky State University, Volgograd, 2019) (in Russian).
[39] V.A. Rassolov, M.A. Ratner, J.A. Pople, P.C. Redfern, L.A. Curtiss. J. Comp. Chem., **22** (9), 976 (2001). DOI: 10.1002/jcc.1058
[40] N. Boroznina, I. Zaporotskova, S. Boroznin, E. Dryuchkov. Chemosensors, **7** (1), 11 (2019). DOI: 10.3390/chemosensors7010011
[41] R.O. Jones. Rev. Mod. Phys., **87** (3), 897 (2015). DOI: 10.1103/RevModPhys.87.897
[42] Y. Yang, J. Wang, Y. Shu, Y. Ji, H. Dong, Y. Li. Phys. Chem. Chem. Phys., **24** (15), 8591 (2022). DOI: 10.1039/D1CP05442B
[43] E. Napiórkowska, K. Milcarz, Ł. Szeleszczuk. Int. J. Mol. Sci., **24** (18), 14155 (2023). DOI: 10.3390/ijms241814155
[44] E.R. Davidson, A.E. Clark. Int. J. Quant. Chem., **122** (8), e26860 (2022). DOI: 10.1002/qua.26860
[45] S.C. North, K.R. Jorgensen, J. Pricetolstoy, A.K. Wilson. Front. Chem., **11**, 1152500 (2023). DOI: 10.3389/fchem.2023.1152500
[46] N.M. O'Boyle, A.L. Tenderholt, K.M. Langner. J. Comp. Chem., **29**, 839 (2008). DOI: 10.1002/jcc.20823

Translated by T.Zorina